Int. J. Solids Structures Vol. 26, No. 9/10, pp. 1037–1069, 1990
Printed in Great Britain.

0020–7683/90 $3.00 + .00

DURABILITY OF STIFFENED COMPOSITE PANELS UNDER REPEATED BUCKLING

TANCHUM WELLER and JOSEF SINGER
Faculty of Aerospace Engineering, Technion—Israel Institute of Technology, Haifa 32000, Israel

Abstract—An experimental study of the durability under repeated buckling of Graphite/Epoxy stiffened panels subjected to shear and axial compression was carried out. The shear panels were hybrid Wagner beams with composite webs bonded to an aluminum alloy frame, whereas the axial compression specimens were "*I*" and "*J*" stiffened cocured composite panels.

The test results demonstrate that composite stiffened panels are less fatigue sensitive than comparable metal ones. In the shear panels repeated buckling, even when causing extensive damage, does not reduce the residual strength by more than 20 percent. For the axial compression panels no reduction in residual strength was observed. Safe design of stiffened Graphite/Epoxy panels well beyond their initial buckling is therefore feasible. This can lead to more efficient structures.

1. INTRODUCTION

Stiffened plates and curved panels are widely used as primary structural elements in aerospace, marine and civil engineering. Their stable postbuckling behavior and their capability to sustain loads far in excess of their initial buckling loads may lead to considerable weight savings, if their postbuckling strength is fully utilized and possible fatigue problems are eliminated.

Stiffened panels loaded in axial compression were extensively studied and employed in aeronautical structures in the thirties, forties and beyond, yielding the "effective width" concept [Von Karman *et al.* (1932), and later also in civil and marine engineering, Faulkner (1975)]. Shear loaded panels were also widely studied and employed by aeronautical engineers in the same period. The stiffeners in aeronautical use were at the time relatively rigid and were analysed with the model of "diagonal tension" (Wagner, 1929), and later by the theory of "incomplete diagonal tension" (Kuhn *et al.*, 1952). During the fifties and sixties, utilization of the stable postbuckling behavior of plates in shear was extended to civil engineering applications, mainly for plate girders (Rockey, 1977, or Ari-Gur *et al.*, 1982). In most civil engineering designs the flanges of the plate girder are relatively flexible and the mode of ultimate failure can be flange collapse rather than web tear.

In the last decade, the trend to optimize the design of shear panels, and the employment of composites and higher strength metals, has led to similar required relative stiffnesses in both civil and aeronautical engineering. The civil engineers employ stiffer flanges in order to improve the postbuckling strength of the web and the aeronautical engineers decrease the relative flange cross-sectional area in order to save weight.

However, airframe failures in service and recent studies (Weller *et al.*, 1984) have revealed that repeatedly buckled stiffened shear panels might be susceptible to premature failure due to fatigue. Local fatigue cracks generated by repeated bending stresses, superimposed on the in-plane shear stresses, initiate near the corners, where the tension diagonal of the buckle interacts with the stiffener. These cracks penetrate through the web thickness and then extend along the stiffeners until final collapse, due to exceeding the plate residual strength, takes place. The danger increases with the number of load cycles, the ratio of working load to the corresponding critical load and the susceptibility of the material to the amplified local stresses, and failure can occur well within the flight envelope loads of airframe.

An extensive investigation was therefore initiated at the Technion Aircraft Structures Laboratory to study the capability of stiffened straight metal shear panels to withstand repeated buckling, far in excess of initial buckling (Ari-Gur *et al.*, 1982; Weller *et al.*, 1984a; Kollet *et al.*, 1983; Libai *et al.*, 1984).

The core of the investigation consisted of instrumented repeated buckling tests on 5 bay "Wagner beams" in a three-point loading system under realistic test conditions (Fig. 1), supplemented by numerical analyses with STAGS (Almroth *et al.*, 1973). The focus was on the influence of the surrounding structure, the stiffeners and on the durability of the panel. Hence the effects of varying sizes of stiffeners, of the magnitude of initial buckling loads, of the panel aspect ratio and of the cycling shearing force, V_{cyc}, were studied. The cyclic to critical shear buckling ratios, (V_{cyc}/V_{cr}), ranged between 2.10 and 9.33, all on the high side as needed for efficient panel design. Yet they were all within possible flight envelopes, with ultimate load ratios, (V_{ult}/V_{cyc}), ranging between 1.84 and 3.68.

The test and numerical results were synthesized in Weller *et al.* (1984) into prediction formulas, which relate the life of the metal shear panels to two cyclic load parameters: the (working/buckling) load ratio, (V_{cyc}/V_{cr}), and the (ultimate/working) load ratio, (V_{ult}/V_{cyc}), which reflects the working load level in the flight envelope, and one geometrical parameter: the (plate/stiffener) stiffness ratio, (b^3t/I_f). It was also found there that the level of shear load, at which local yielding first takes place, V_y, dominates the endurance of the panel, and hence the life predictions could be expressed in a simpler manner, in terms of a single load ratio, (V_{cyc}/V_y).

It was concluded that for metal shear panels the number of cycles to crack initiation and to failure are mostly affected by the (ultimate/working) load ratio. In the life prediction formula this fact is evidenced by the exponent of (V_{ult}/V_{cyc}) being 5 times or more that of (V_{cyc}/V_{cr}). It was also pointed out that boosting the working load by increasing the relative stiffness of the frame might lead to degradation in fatigue life for a prescribed (ultimate/working) load ratio. This deterioration stems from the local effects of stiffener rigidity on the stress concentrations near the corners of the panel where the diagonal-tension buckle interacts with the stiffeners. Thus far the evidence from metal shear panels.

With the increasing employment of composite structural elements in aerospace vehicles their repeated buckling behavior has become of primary importance. At present, due to the scarcity of sound and adequate data on postbuckling behavior, durability and fatigue failure modes of buckled composite structural elements, composite panel design is rather conservative and prohibits buckling within the flight envelope. For more efficient composite structures, that fully utilize their large potential advantage over metal structures, designs must however include postbuckling states of loading. Hence, research work has been initiated in the last decade to build up the essential understanding and data. Studies on postbuckling and repeated buckling of composite shear panels, most of which combine experiments and analysis, have been reported in Vestergren *et al.* (1978), Renieri *et al.* (1981a), Agarwal (1981), Kudva *et al.* (1981), Deo (1985), Deo *et al.* (1985) and Rouse (1987). Similar investigations on axially loaded composite panels are presented in Deo (1985), Deo *et al.* (1985), Spier (1975), Renieri *et al.* (1981b), Agarwal (1982), Knight *et al.* (1985), Starnes *et al.* (1985), Romeo (1986) and Bushnell (1987). These studies have demonstrated the great weight saving potential of composite panels, but have also pointed out the necessity for additional extensive investigations essential for realization of this potential. The Technion group has also been part of this effort (Weller *et al.*, 1984; Segal *et al.*, 1987; Frostig *et al.*, 1988, 1989).

It has been recognized in these studies on composite panels (Weller *et al.*, 1984), as in the earlier work on metal panels, that the postbuckling problem is highly nonlinear and its solution requires the details of overall stress distributions at working loads and in particular, specific knowledge of the high stresses which, as in metal panels, may here lead to fatigue problems in regions where buckles of skin interact with stiffeners. Although large computer programs nowadays contain sophisticated nonlinear capabilities, their employment for performing a routine nonlinear detailed analysis is as yet extremely complicated for realistic stiffened panels, prohibitively expensive and hence unrealistic from computational and design aspects. On the other hand, analytical approaches, such as energy methods (Kudva *et al.*, 1981), are confined to approximate determination of some of the more important general parameters pertinent to the deformation pattern. They are, therefore, insufficient for the detection of the high stress concentration discussed above, and thus ignore the cardinal initiator of fatigue problems.

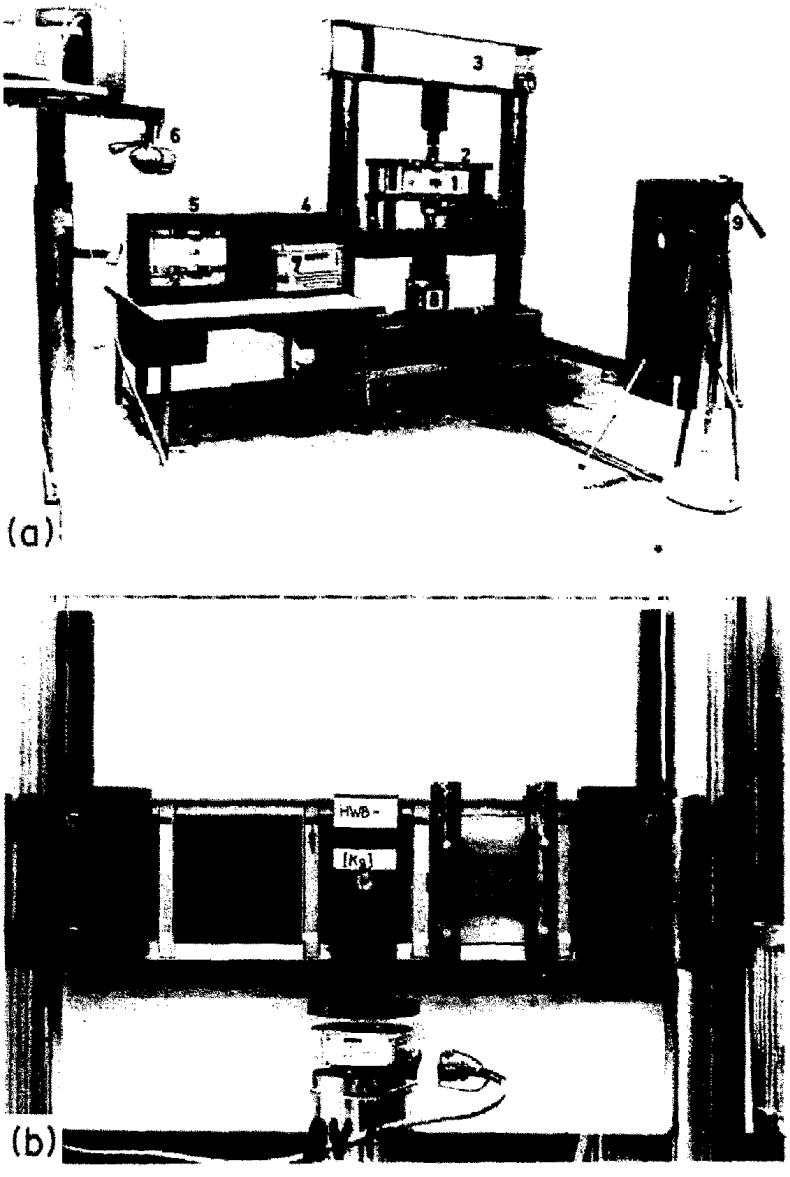

Fig. 1a. Test setup (Weller *et al.*, 1984a). 1—Test specimen. 2—Cross members for lateral displacement prevention. 3—Loading frame. 4—Video recorder. 5—T.V. monitor. 6—Moiré lamp. 7—Multichannel data logger. 8—MTS hydraulic jack. 9—Cameras.

Fig. 1b. New loading rig.

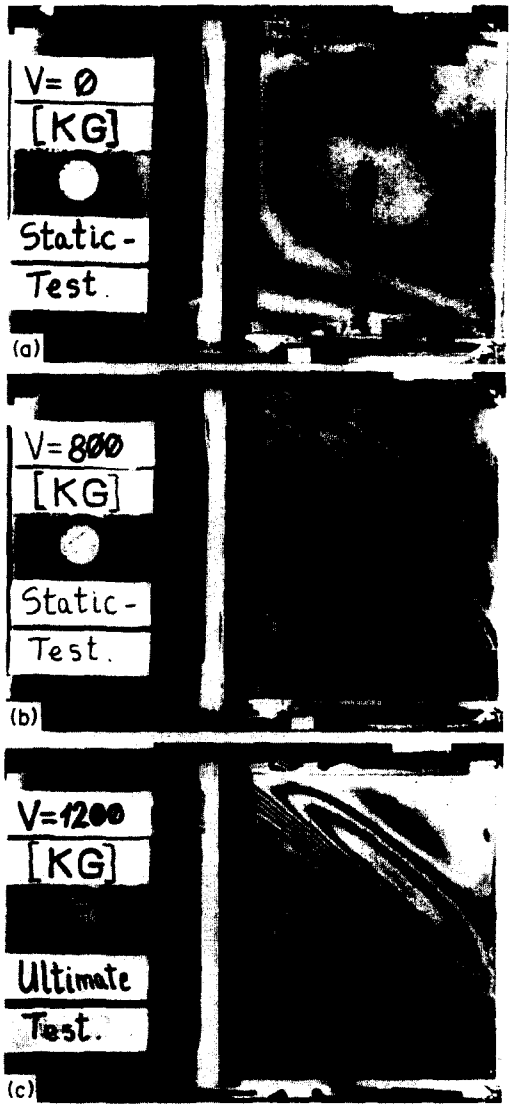

Fig. 4. Static test of shear web HWB-01—Moiré fringe pattern. (a) Web-HWB-01B, $V = 0$ kg. (b) Web-HWB = 01B, $V = 800$ kg. (c) Web-HWB-01A, $V = 1200$ kg.

Obviously, when very detailed information is required, numerical methods and large computer codes cannot be avoided. Some calculations used for comparisons with tests and fatigue analysis have been documented in Renieri *et al.* (1981a), Agarwal (1981), Kudva *et al.* (1981) and Segal *et al.* (1987). It should, however, be noted that the requirements for inelastic and extremely high strains and stresses are usually difficult to satisfy and available programs do not handle postbuckling responses satisfactorily, in particular of composite structures.

Additional combined experimental and analytical studies of the postbuckling response of composite structures, in particular the behavior of repeatedly postbuckled composite stiffened panels, are therefore urgently needed. This motivated the initiation of a research program at the Technion Aircraft Structures Laboratory to demonstrate the feasibility of loading composite stiffened panels safely well into the postbuckling region and their capability to withstand many repeated "deep" buckles before failure occurs, or to show their low fatigue sensitivity. Some preliminary results related to shear loading which fulfill these expectations have been presented in Weller *et al.* (1984b). Studies on panels, with "*I*" and "*J*" shape stiffeners, subjected to axial compression, reported in Segal *et al.* (1987) and Frostig *et al.* (1988, 1989), have also verified the expected low fatigue sensitivity and have demonstrated that, contrary to previous studies in Knight *et al.* (1985) and Starnes *et al.* (1985), no debonding of stiffeners occurred. In the present study, the investigations of Weller *et al.* (1984a), Segal *et al.* (1987) and Frostig *et al.* (1988, 1989) have been further pursued and evaluated in order to provide necessary data for design of efficient stiffened composite structures.

The results of the shear loading studies are presented here in detail, whereas those of the axial compression studies are only briefly summarized, and the details appear in Segal *et al.* (1987) and Frostig *et al.* (1988, 1989).

2. TEST SETUP AND PROCEDURES

2.1. *Shear loading*

Two main considerations: realistic test conditions and relatively high load ratios compared with buckling, have influenced the choice of the test configuration and corresponding parameters in the present studies. These considerations were discussed in detail in Weller *et al.* (1984a) and Libai *et al.* (1984) and led to a three-point-loading Wagner beam test configuration, which has also been adopted in the present studies. The test setups employed for this test configuration have been described in detail in Weller *et al.* (1984a) and Weller *et al.* (1984b) and are shown in Figs 1a and 1b. It should be noted that due to apparent differences in rigidities of the two frames of Fig. 1 all ultimate tests were conducted in the same frame, that of Fig. 1a, thus eliminating any possibility of introducing frame stiffness effects on the ultimate strength of the beams.

The response of the specimens was measured by strain gage rosettes bonded face to face to the web of the beam. The gages were located according to Fig. 3. The strains measured by the gages were recorded by a multichannel data logger. The laminated construction of the web necessitated some "on line" calculations during the course of loading the beam to determine the principal strains as well as stress levels for each lamina. This assisted in detecting (only theoretically) any possible "local" failure mode due to reaching, or exceeding, the composite allowables in any particular lamina. A simple computer code was used to process the strain readings and furnish the lamina principal elastic strains and stresses.

In addition to the strain gage measurements, the shadow Moiré technique was employed for global observation of the deflected pattern of the web on the way to and during buckling, and in the postbuckled region (see Figs 4a to 4c, note that the "Dummy" plate is introduced either to protect or to replace one of the test webs). The grids used in the technique were removed whenever damage was expected to initiate, or the deflections of the web became significant to permit a visual detection of crack initiation and its progress, and to avoid damage of the grids due to beam failure. The technique was also used to track "dynamic" damage propagation of the web as reflected by a continuous change of the deflected pattern of the web, whenever possible (see Figs 6a to 6c).

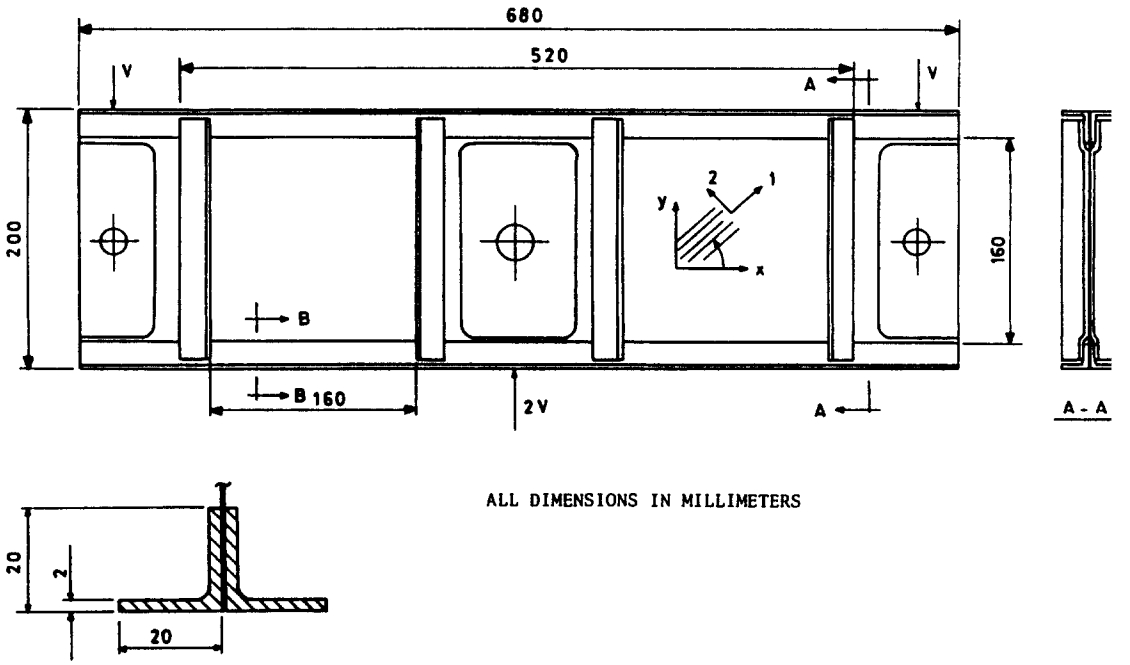

Fig. 2. Hybrid Wagner beam of test series.

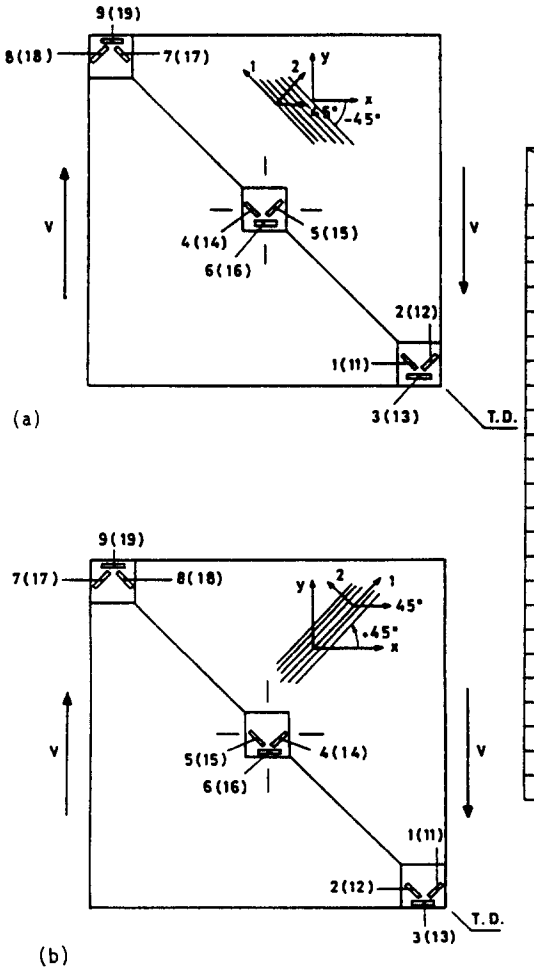

WEB / HMB \ GAGE	11	12	13	14	15	16	17	18	19
	1	2	3	4	5	6	7	8	9
01 A	x	x	x	x	x	x	x	x	x
01 B	x	x	x	x	x	x	x	x	x
02 A	x	x	x	x	x	x	-	-	-
02 B	x	x	x	x	x	x	-	-	-
03 A	x	x	x	x	x	x	-	-	-
03 B	x	x	x	-	-	-	-	-	-
04 A	x	x	-	x	x	-	-	-	-
04 B	-	-	-	x	x	-	-	-	-
05 A	x	x	-	x	x	-	-	-	-
05 B	-	-	-	x	x	x	-	-	-
06 A	x	x	-	x	x	-	-	-	-
06 B	x	x	-	x	x	-	-	-	-
07 A	x	x	-	x	x	-	-	-	-
07 B	x	x	-	-	-	-	-	-	-
08 A	x	x	-	x	x	-	-	-	-
08 B	x	x	-	x	x	-	-	-	-
09 A	x	x	-	x	x	-	-	-	-
09 B	-	-	-	x	x	-	-	-	-
10 A	x	x	-	x	x	-	-	-	-
10 B	-	-	-	x	x	-	-	-	-
11 A *	x	x	x	x	x	x	-	-	-
11 B *	x	x	x	-	-	-	-	-	-
12 A *	-	-	-	x	x	x	-	-	-
12 B *	-	-	-	x	x	x	-	-	-

(BACK)
(FRONT)

* see TENSION case (a)

Fig. 3. Strain gages location. (a) Outermost fibres in tension. (b) Outermost fibres in compression.

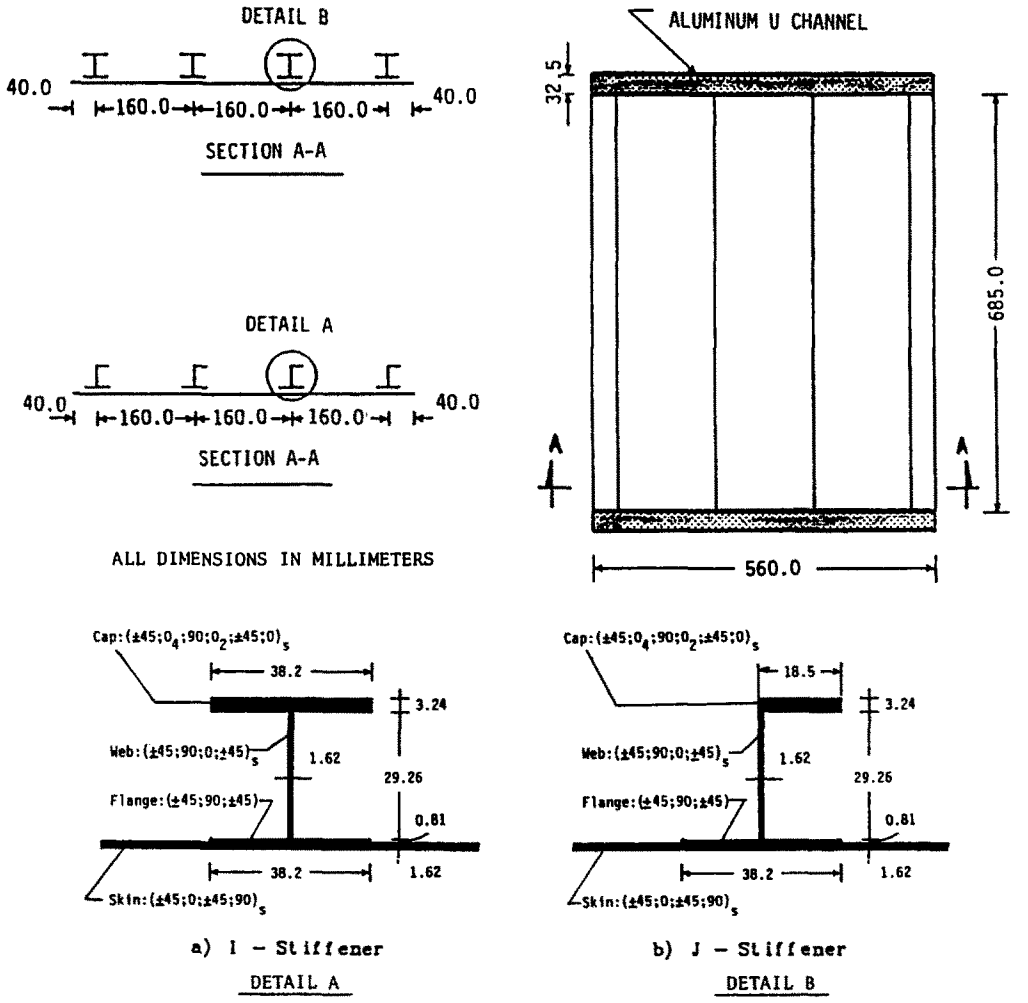

Fig. 5. Axial compression panels geometry and dimensions.

As a result of adopting the test configuration and test rigs of Weller *et al.* (1984a) and Weller *et al.* (1984b), the configuration and dimensions of the present Graphite Epoxy beams were similar to the metal ones of Weller *et al.* (1984a) (see Fig. 2). Consequently, the test procedures also followed those of Weller *et al.* (1984a). It should however be noted that, though (as earlier in Weller *et al.* (1984a)) each beam provided two different tests, testing of the second test section, after failure of the first one, could not be performed here in the inverted position employed for the metal beams (discussed in detail in Weller *et al.* (1984a)). Here the position of the beam in the loading frame dictates the state of stress, either compression or tension, in the fibers in the outermost laminae of the web in the present beams. As has been indicated in Weller *et al.* (1984b), this affected the test results significantly, because the modes of failure and fatigue strength, the residual strength and ultimate strength are all dependent on the state of stress in the outermost fibers.

Following Weller *et al.* (1984a), each web, except those tested for ultimate strength, was tested according to the following phases:

(a) Buckling strength—the beam was loaded gradually to determine its actual critical load.
(b) Postbuckling and fatigue strength—the load was further increased until lamina strains, measured or calculated "on line" as explained before, reached a predetermined strain level, or indicated a possible failure mode due to reaching or exceeding the material allowables. The load reached at this stage constituted the maximum working load level for the following fatigue studies V_{cyc}. The load was released and the gages and Moiré pattern were recorded to detect any residual strains or deflections due to loading into the postbuckling region.

Henceforth the test consisted of continuous repeated loading at a very low frequency (~ 2 Hz) between zero shear loading, $V = 0$ and V_{cyc}. This phase was aimed at determining the fatigue strength under the prescribed load level. Loading of the beam was interrupted every few thousand cycles for complete strain gage records (as long as the gages had not been fatigue damaged) and Moiré records, and for detection of initiation of failure. Once failure was observed, or predicted by the "on line" calculations, its further propagation was continuously measured by the gages and processed until gage failure occurred (see Fig. 6 of Weller *et al.* (1984b)). A concurrent procedure was the monitoring and recording of the changes in the Moiré patterns by a video camera and tape, if possible (see Figs 6a–6c).

This phase continued until either substantial damage of the web was observed, or the number of cycles reached a predetermined value (250 K cycles in the present studies). It should be noted that at this stage, the specimen was either damaged or "intact".

(c) Residual strength—a static ultimate test was conducted with each specimen that underwent the cyclic/fatigue stage. This aimed at determining the effect of apparent modes of damage on the load carrying capacity of the damaged beam, or the existence of an effect of repeated buckling on the "intact" beams. Neither strain measurements nor Moiré patterns were recorded during this phase.

In order to determine the loading ratio of the web, (V_{cyc}/V_{ult}), and study the fatigue "sensitivity" of the beam, as reflected by its residual strength, ultimate strength tests were carried out for each web configuration and position of the beam in the loading fixture, i.e. outermost external fibers either in tension or compression. In these tests "virgin" specimens were gradually loaded to determine their actual static ultimate load.

2.2. *Compression loading*

In order to achieve the main objectives of the present study: (a) postbuckling behavior of stiffened Graphite-Epoxy panels subjected to uniform axial compression and (b) evaluation of the influence of "deep" repeated buckling on the buckling and postbuckling behavior, and on the failure modes of stiffened panels, relatively heavy "*I*" and "*J*" shape stiffeners were selected for the panels, which were tested in compression in a 50 ton MTS test machine.

The test specimens were instrumented with multiple pairs of strain gages bonded back-to-back, used to detect incipient skin buckling and to measure the strain levels during the test (Segal *et al.*, 1987). The patterns of the out-of-plane displacements were also recorded with a Moiré shadow fringe technique (see Fig. 18).

Loading procedures were similar to those of the shear beams in Section 2.1, and the load levels which ranged from about 1.5 times the initial local buckling load corresponding to the panel and up to about 0.7 of its ultimate strength (sustained by the reference panel). The tests were performed at room temperature on specimens which had no moisture conditioning.

3. TEST SPECIMENS

3.1. *Shear specimens*

Tests were conducted with four groups of shear beams. This provided 12 beams with 24 test web sections. The dimensions and configuration of the beams are shown in Fig. 2. The beams were of a hybrid type construction, 2024 T3 aluminum frame bonded to composite webs of either T300/5208 Gr/Ep tapes, or Gr/Ep planeweave 5302/3K-70-PW/AS4. The frames of the beams in all groups were identical and consisted of identical "*L*" section uprights and flanges $-L\ 20 \times 20 \times 2\ \text{mm}^3$. The webs were composed of unidirectional plies stacked in $[+45\,;\,-45]_s$, $[+45\,;\,-45\,;\,\bar{0}]_s$, and $[+45\,;\,-45\,;\,90\,;\,\bar{0}]_s$, layups and planeweave stacked in the $[\underline{\pm 45}]_s$ layup (see Table 3). The mechanical properties of the unidirectional tapes and planeweave are given in Table 1.

The stiffeners were bonded to the web in a specially designed template by EA-9309.1 adhesive (Hysol comp., IAI code) and cured in a vacuum bag at room temperature to avoid

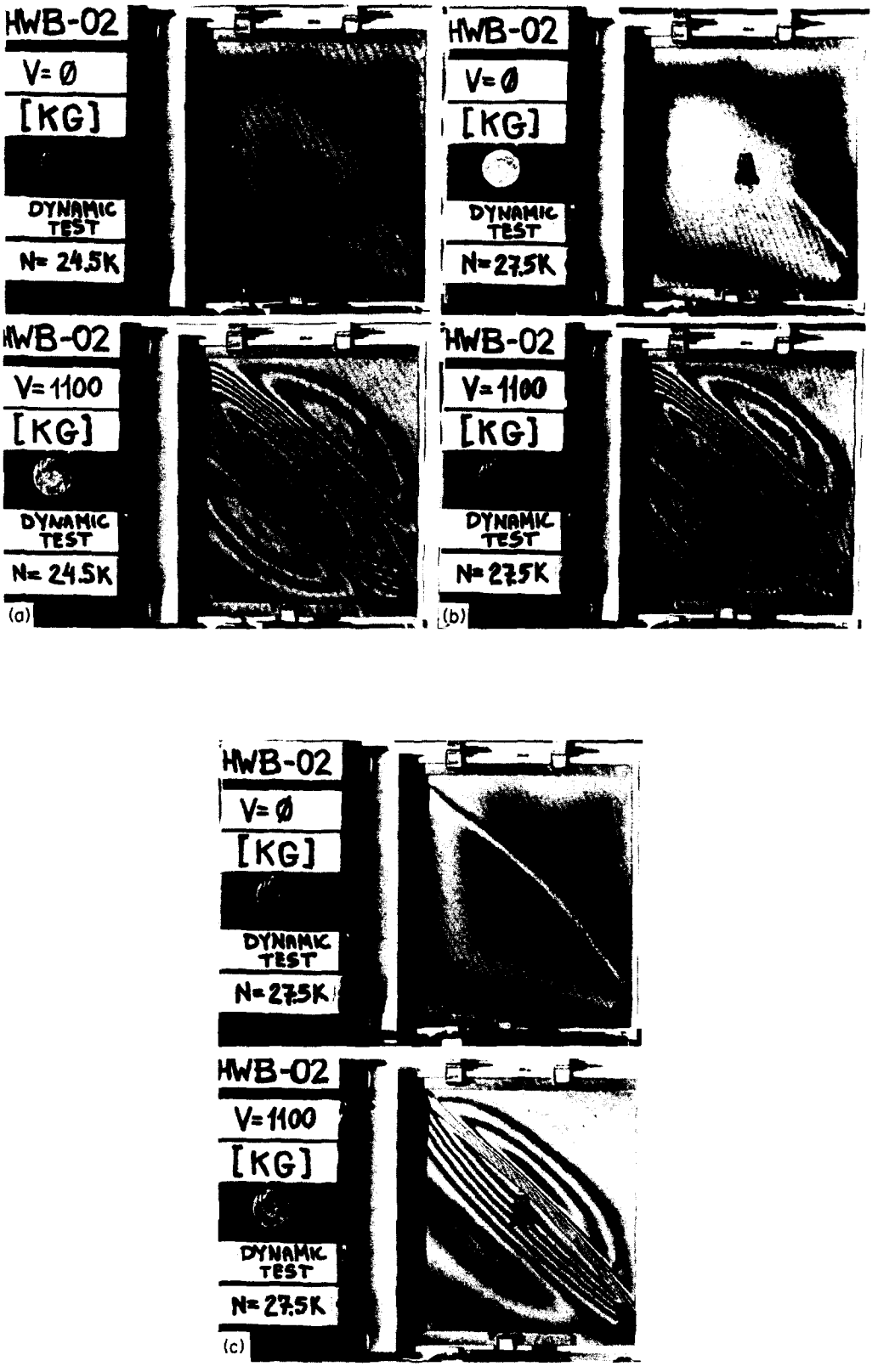

Fig. 6. Dynamic test of shear web HWB-02A—Moiré fringe patterns of dynamic damage propagation, at $V = 0$ and $V = 1100$ kg. (a) $N = 24{,}500$ cycles. (b) $N = 27{,}500$ cycles. (c) $N = 27{,}500$ cycles, after complete failure.

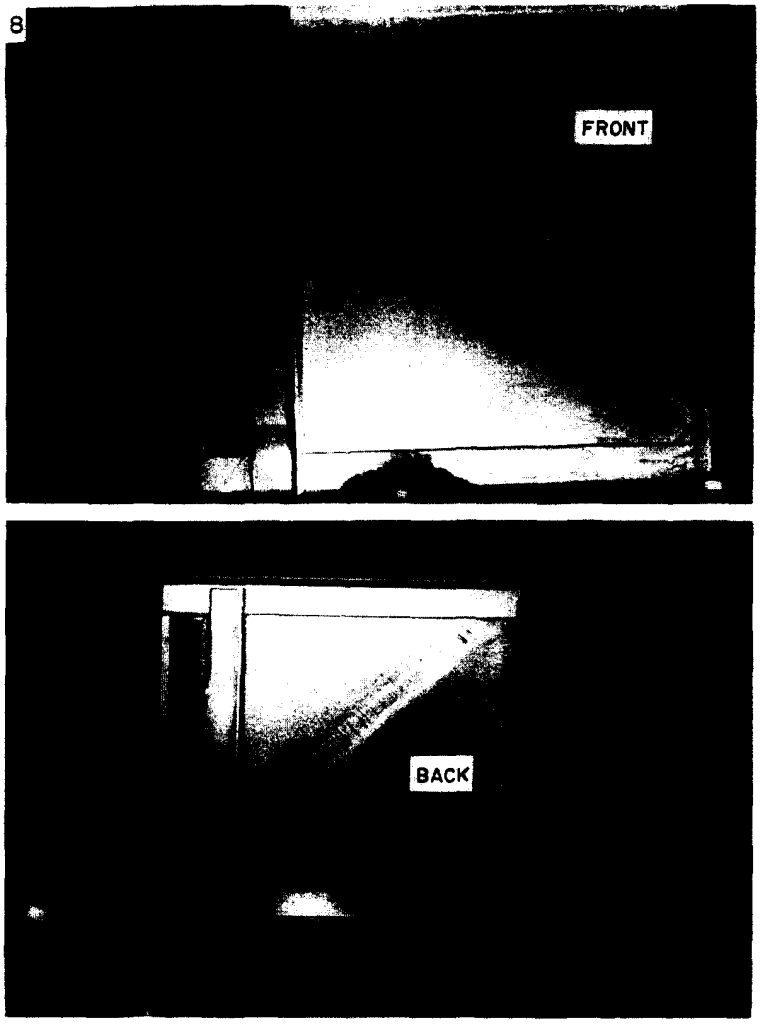

Fig. 8. Damaged shear web HWB-02A.

Table 1. Composite materials moduli

Modulus \ Material	Gr/Ep T3000/5208	Gr/Ep planeweave 3502/3K-70-PW/AS4	Gr/Ep AS4/3502
E_{11}[kg/mm^2]	15,000	6740	13,360
E_{22}[kg/mm^2]	1,000	6650	930
G_{12}[kg/mm^2]	600	560	580
ν_{12}	0.27	0.05	0.34
F_{1T}[kg/mm^2]	150.0	65.6	145.5
F_{1C}[kg/mm^2]	140.0	56.5	149.3
F_{2T}[kg/mm^2]	6.0	58.6	4.7
F_{2C}[kg/mm^2]	26.0	51.0	23.9
F_{12}[kg/mm^2]	8.0	10.2	7.2
F_{13}[kg/mm^2]	—	4.8	11.0

compatibility problems between the aluminum stiffeners and composite web. The controlled bonding and procedures were developed by Israel Aircraft Industries and comply with aircraft standards, so as to be able to sustain the load spectrum and modes planned for the program.

Pairs of strain gage rosettes were bonded face to face along the tension diagonal (Fig. 3). Gages were located adjacent to the corners, where the buckle of the web interacts with the stiff frame and high local stresses, which might lead to fatigue problems, develop, and at the center of the web to detect incipient buckling, as well as to evaluate the average overall behavior of the web.

Since the present test program was based on the considerations, as well as the results of Weller *et al.* (1984a), the dimensions of the beams were chosen in a manner that would allow comparison of the results and conclusions of Weller *et al.* (1984a) with those experienced and concluded in the present studies.

3.2. *Axial compression stiffened panels*

Both panel configurations consisted of a 12 ply skin stiffened by four equally spaced longitudinal "*I*" or "*J*" type stiffeners. Each stiffener had a web of 12 plies and cap of 24 plies. The layup and stacking sequence of the skin and stiffeners are presented in Table 2. The panels were fabricated from AS4/3502 Graphite/Epoxy tapes (see Table 1). The geometry and dimensions of the panels are shown in Fig. 5.

The panels were designed and fabricated at Israel Aircraft Industries, Engineering Division. The manufacturing process consisted of a single curing cycle with the stiffeners integrally laid into the skin and cocured with it. To ensure uniform loading of the panel, the ends were cast into an aluminum *U* shaped channel using an epoxy-resin mixed with glass fibers. Then the loaded surfaces of these *U* channels were machined flat and parallel to each other.

4. RESULTS AND DISCUSSION

4.1. *Shear beams*

The test results yielded by the four groups of shear beams, studied in the present program, appear in Table 3, together with the state of loading under which the tests have been performed. (*T* indicates loading that results in tensile stresses in the external fibers and *C* loading that yields compressive stresses there.) The buckling shear loads, corresponding to

Table 2. Panel layup orientation and sequence

Configuration	Skin	Stiffener web	Stiffener cap
"*I*" stiffener	$(\pm 45, 0, \pm 45, 90)_s$	$(\pm 45, 90, 0, \pm 45)_s$	$(\pm 45, O_4, 90, O_2 \pm 45, 0)_s$
"*J*" stiffener	$(\pm 45, 0, \pm 45, 90)_s$	$(\pm 45, 90, 0, \pm 45)_s$	$(\pm 45, O_4, 90, O_2 \pm 45, 0)_s$

O: Orientation denotes plies layed with fibers running longitudinally.

Table 3. Shear beams—test results

Web lay up	Web No.	State of stress external fibers	Critical loading of web		Dynamic test No. 1		
			$(V_{cr})_{cal}$ kg	$(V_{cr})_{exp}$ kg	V_{cyc} kg	V_{cyc}/V_{ult} I & II	N K cycles
$(+45; -45)_s$	01A	T	32	<30	500	0.174/0.167	95
	01B	T	32	<30	800	0.278/0.267	400
	02A	C+T	92(C)	85	1.100(C)	0.550/0.431	27.5
	02B	C	92	85	—	—	—
	03A	C	92	80	800	0.400/0.314	250
	03B	C	92	—	1.000	0.500/0.392	120
	04A	T	32	<26	1.100	0.383/0.367	250
	04B	T	32	—	1.200	0.417/0.400	184
$[+45; -45; \bar{0}]_s$	05A	T	75	<100	1.100	0.330/0.329	250
	05B	T	75	—	—	—	—
	06A	C	165	<140	1.100	0.431/0.389	250
	06B	C	165	<150	1.300	0.510/0.459	250
	07A	C	165	<160	1.500	0.588/0.530	250
	07B	C	165	—	—	—	—
$(+45; -45; 90; \bar{0})_s$	08A	C	368	<320	2.000	0.615/0.513	41.74
	08B	C	368	—	1.700	0.523/0.436	260
	09A	C	368	<325	1.850	0.569/0.474	252.8
	09B	C	368	<500	—	—	—
	10A	T	230	<150	1.850	0.536/0.578	250
	10B	T	230	<450	—	—	—
$(\pm\underline{45})_s$	11A	—	32	—	1.000	0.444	250
	11B	—	32	—	900	0.400	250
	12A	—	32	—	1.250	0.556	250
	12B	—	32	<120	—	—	—

Web lay up	Web No.	State of stress external fibers	Dynamic test No. 2			Ultimate test load	
			V_{cyc} kg	V_{cyc}/V_{ult} I & II	N K cycles	$(V_{ult})_I$ kg	$(V_{ult})_{II}$ kg
$(+45; -45)_s$	01A	T	—	—	—	2.875	3.000
	01B	T	—	—	—	—	—
	02A	C+T	1.100(C) 1.100(T)	0.383/0.367	70 30	—	—
	02B	C	—	—	—	2.000	2.550
	03A	C	900	0.450/0.353	35	—	—
	03B	C	—	—	—	—	—
	04A	T	—	—	—	—	—
	04B	T	—	—	—	—	—
$[+45; -45; \bar{0}]_s$	05A	T	1.300	0.390/0.388	250	—	—
	05B	T	—	—	—	3.330	3.350
	06A	C	1.300	0.510/0.459	250	—	—
	06B	C	—	—	—	—	—
	07A	C	—	—	—	—	—
	07B	C	—	—	—	2.550	2.830
$(+45; -45; 90; \bar{0})_s$	08A	C	—	—	—	—	—
	08B	C	—	—	—	—	—
	09A	C	—	—	—	—	—
	09B	C	—	—	—	3.250	3.900
	10A	T	—	—	—	—	—
	10B	T	—	—	—	3.450	3.200
$(\pm\underline{45})_s$	11A	—	—	—	—	—	—
	11B	—	—	—	—	—	—
	12A	—	—	—	—	—	—
	12B	—	—	—	—	2.250	2.250

Table 3. (*continued*)

Web lay up	Web No.	State of stress external fibers	Residual strength I $(V_{res})_I$ kg	I $V_{res}/(V_{ult})_{II}$	II $(V_{res})_{II}$ kg	II $V_{res}/(V_{ult})_{II}$	III $(V_{res})_{III}$ kg	III $V_{res}/(V_{ult})_{II}$
$(+45; -45)_s$	01A	T	2.875	0.958	3.000	1.000	—	—
	01B	T	2.340	0.780	2.520	0.840	—	—
	02A	C+T	2.180(C)	0.855	—	—	—	—
	02B	C	—	—	—	—	—	—
	03A	C	2.180	0.855	2.000	0.784	1.870	0.733
	03B	C	2.730	—	2.950	—	—	—
	04A	T	2.420	0.807	2.510	0.837	—	—
	04B	T	1.300	0.433	1.400	0.467	—	—
$(+45; -45; \bar{0})_s$	05A	T	1.910	0.570	2.860	0.854	3.070	0.916
	05B	T	—	—	—	—	—	—
	06A	C	2.300/2.500	0.883	2.750	0.972	2.880	1.018
	06B	C	2.300	0.813	2.700	0.954	3.000	1.060
	07A	C	1.930	0.693	2.880	1.018	3.250	1.148
	07B	C	—	—	—	—	—	—
$(+45; -45; 90; \bar{0})_s$	05A	C	3.630	0.931	—	—	—	—
	08B	C	3.100	0.795	3.200	0.821	3.480/3800	0.974
	09A	C	3.210	0.823	3.290	0.844	—	—
	09B	C	—	—	—	—	—	—
	10A	T	2.750	0.859	3.000	0.938	—	—
	10B	T	—	—	—	—	—	—
$(\underline{\pm 45})_s$	11A	—	2.000	0.889	—	—	—	—
	11B	—	2.250	1.000	—	—	—	—
	12A	—	2.160	0.960	1.750	0.778	—	—
	12B	—	—	—	—	—	—	—

(T) : outermost fibers in tension.
(C) : outermost fibers in compression.

each type of web and state of loading are also given in this table. These critical loads were calculated with Eqn (4.84) of Ashton *et al.* (1970), which corresponds to simply supported boundary conditions along the edges of the web, and were then "corrected" to account for the stiffening effect of the frame, following the procedures of Kuhn *et al.* (1952). It should, however, be noted that the critical loads are presented for reference purposes only, as explained in the discussion below, and already pointed out in Weller *et al.* (1984b).

It should also be clarified that the working load levels, V_{cyc}, have been chosen in compliance with the requirement that no lamina should experience a tension strain exceeding 1% at the points of strain measurements.

The first group of results in Table 3 is related to the beams with $[+45; -45]_s$ composite webs (beams HWB-01 to HWB-04). Most of the results pertinent to these beams, HWB-01 to HWB-03, have already been presented and discussed in the preliminary report of Weller *et al.* (1984b). Like beam HWB-01 the additional beam, HWB-04, has been positioned in the loading frame with the outermost fibers in a tension state of loading. As anticipated, this results in a low critical load, $(V_{cr})_{exp} < 26$ kg. It was pointed out in Weller *et al.* (1984b) that precise determination of such a low value of buckling load could not be achieved with the present frame loads, since at this load level any strain/strain, or load/strain response reduced from the strain gages (be it bending vs. membrane strain, bending/membrane strain vs. applied load or direct strain measurements vs. applied load) was inadequate for determination of the critical load (see for example Fig. 7 of Weller *et al.* (1984b)). This problem of experimental buckling load determination requires further investigation.

It is observed in Table 3 that the webs of beam HWB-04 were subjected to significantly higher working load ratios, (V_{cyc}/V_{ult}), than those of the corresponding beam HWB-01. As can be seen from Table 3, these higher working load levels had almost no influence on the durability and residual strength of web 04A (as compared with web 01B). They affected severely, however, the damage formation, cracks and delaminations at the lower corner of

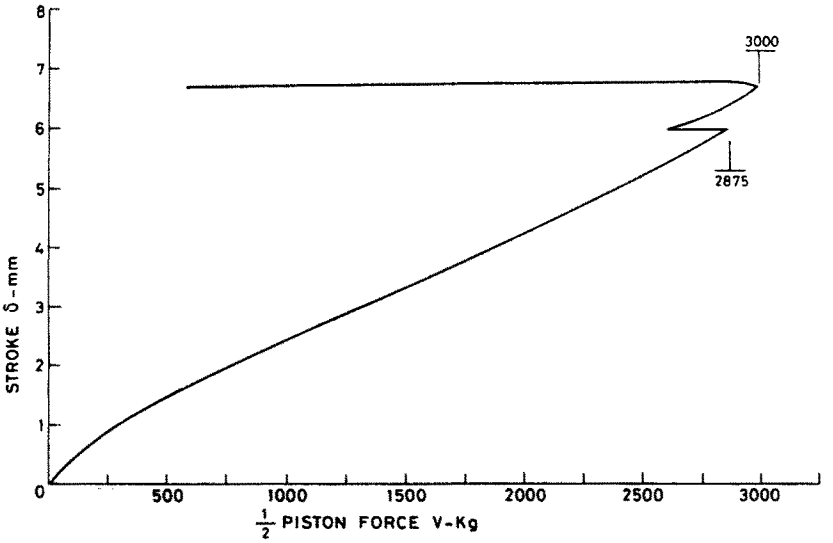

Fig. 7. MTS stroke vs load in ultimate test, web HWB-01A.

the tension diagonal, T.D. (where frame flanges are in compression) of web 04B. Damage of this web had already been fully developed at $N = 184$ K cycles—and was characterized by complete matrix cracking along the T.D. The residual strength test, following the repeated buckling test (of 184 K cycles), yielded very low residual strength values compared with either web 01B or 04A. It should be noted that failure of web 04B was associated with pronounced simultaneous damage of the frame, which might have led to premature web failure. The stiffness behavior of the webs of beam HWB-04 was similar to that of the webs of beams HWB-01 to 03 (see Fig. 7 and Weller *et al.* (1984b)).

Beams HWB-02 and 03 were loaded with their outermost fibers in a state of compression. This resulted in higher buckling loads, but in more pronounced damages in the form of cracks and delamination at the lower corner of the T.D., and also reduced ultimate loads (see Table 3, and Weller *et al.* (1984b)).

A peculiar composite behavior was observed in the tests on web 02A. The web was loaded with 1100 kg and damages initiated at $N = 24.5$ K cycles (see Fig. 6a). Cyclic loading of the beam was continued and a steady fast increase of the delamination was observed. The extent of this damage is shown in Fig. 6b for $N = 27{,}500$ cycles. At this stage of cyclic loading, the working load of the MTS machine was set by mistake to 1650 kg rather than 1100 kg. As a result of this, damage spread immediately along the whole length of the tension diagonal (see Fig. 6c). (Additional figures showing intermediate phases of the damage progress are given in Weller *et al.* (1984b)). Obviously this mode of failure of the web could have been declared as total failure at this point. However, it was decided to continue the cyclic loading test with the beam at the previously determined working load of $V_{cyc} = 1100$ kg, in order to examine the effect of such a severe damage on the residual fatigue life of the web. Repeated buckling of the beam was continued up to 70,000 cycles, but no further extension of damage was observed. The final damage pattern of this web is shown in Fig. 8.

One should bear in mind that the above peculiar behavior of the beam was associated with a case where the fibers in the external laminae were in a compression state of stress. Actual flight structures might be exposed to a reversal in state of stress, i.e. tension in the fibers. It was therefore decided to reverse the loading condition of the beam and study the effect of the above damage on the residual fatigue life of the beam under the new loading condition. Cycling of the beam with $V_{cyc} = -1100$ kg (but now in the reverse loading condition) continued for another 30,000 cycles, but no further damage of the beam could be detected.

At this stage the fatigue tests of the beam were terminated and a static residual strength

test was performed. In this test the beam was again loaded with the outermost buckled fibers in compression. The behavior of the beam on the way to failure is shown in Fig. 14 of Weller *et al.* (1984b). The residual strength obtained for this beam was $V_{res} = 2180$ kg. This load is of similar magnitude to the ones obtained for the undamaged webs. Hence, in spite of the severe damages and the tough "punishment" that the web experienced, its residual strength was almost "intact". This may be explained by the capability of the fibers in the internal laminae, which were in a tensile state of the stress, to carry most of the load, when subjected to the present type of shear loading. It is thus concluded that as long as these fibers stay intact, they will provide most of the strength of the beam, practically unaffected by the extent of the damage in the web.

To conclude the discussion on the present group of beams, it is worthwhile noting that degradation in the load carrying capacity due to fatigue of the beams, as reflected by their residual strength, V_{res}, did not exceed 20% for any web tested in the present group, i.e. their fatigue "sensitivity" is relatively low, or their damage tolerance is very good, thus providing a high margin of safety.

The second group of test specimens consisted of 3 beams with $[+45; -45; \bar{0}]_s$ composite webs (beams HWB-05 through HWB-07). As shown in Table 3, the correlation between the calculated and experimental buckling loads is good for this group.

The outermost fibers of the webs of the first beam of this group were in a state of tension. The first web 05A of the beam was cycled at a working load $V_{cyc} = 1100$ kg and sustained its fatigue life of 250 K cycles with no apparent damage. This has also been confirmed by X-raying and acoustic examinations performed after the tests by Israel Aircraft Industries. The working load level was then increased to 1300 kg and again the web sustained its designed fatigue life of 250 K cycles, however now with minor damages in the form of matrix cracking along the T.D. It is observed in Table 3 that when compared with the undamaged nonfatigued web 05B, the residual strength of web 05A was only slightly affected by the two blocks of fatigue loading it underwent. The behavior of web 05A on the way to failure and at failure differed, however, from that of web 05B.

The other two beams, 06 and 07, in this group were loaded with their outermost fibers in a state of compression. Web 06A was subjected to two complete blocks (250 K cycles each) of constant amplitude fatigue loading, one at 1100 kg and the second at 1300 kg. The first block of cyclic loading was associated with minor damages at the upper and lower corners of the T.D. In the second block of loading slight propagation of the damages was observed (see Fig. 9). It is apparent from Table 3 that the two blocks of repeated buckling had almost no influence on the residual strength of the web, when compared with the loads sustained by the "nonfatigued" web 07B. The behavior of web 06A on the way to failure and at failure was, however, different from that of web 07B and resembled that of web 05A, thus being also different from that observed for the webs in the first group of specimens.

Web 06B also sustained its designed fatigue life. No damages were observed during the course of fatigue loading and no residual strength degradation due to fatigue was observed. The behavior on the way to failure and at failure was similar to that of web 06A (see Table 3).

Web 07A was subjected to a relatively high working load level, $(V_{cyc}/V_{ult}) \approx 0.588$. As a result of this, significant cracks developed and propagated during the first quarter of the life of the web. The damage was arrested at about 60 K cycles and the web withstood its complete fatigue envelope (250 K cycles). No fatigue effects on the residual strength of the web were experienced. The behavior of the web on the way to failure and at failure again resembled that of webs 06A and 06B and differed from that of web 07B.

Web 07B was used to determine the ultimate load of the corresponding web layup and state of loading (webs 06A, 06B and 07A). Its modes of failure are shown in Fig. 10.

Typical response curves, yielded by reduction of the strain gage measurements are shown in the sets of Figs 11a–11e (web 06A). It is apparent from these figures that buckling cannot be determined uniquely from these figures. One should also note the very high bending strain concentrations along the tension diagonal at the lower corner of the T.D. which are reflected by the (Y_2/Y_5) curve in Fig. 11e.

Similar sets of response curves and trends of behavior were obtained for the

other webs in the second group, as well as for the first group of webs (beams HWB-01 to HWB-04).

It is also concluded from the results of Table 3 that adding the 0° ply to the web in the second group significantly increased the load carrying capacity (buckling and ultimate strength), and almost eliminated the fatigue sensitivity of the webs. It also changed the behavior of the webs in this group, on the way to failure and at failure, when compared with that observed in the residual strength tests of the first group.

The third group in the present investigations consisted of beams with $[+45; -45; 90; \bar{0}]_s$ composite webs (beams HWB-08 through HWB-10). Table 3 shows that buckling loads corresponding to the webs of this group were increased significantly by the addition of the two 90° laminae. Again, however, though the anticipated buckling loads were relatively high, the experimental determination of the critical loads did not yield unique results and correlation with analysis is less than fair.

The first two beams (HWB-08 and 09) in this group were loaded with the outermost fibers of the webs in compression. Web 08A was subjected to a very high working load, $(V_{cyc}/V_{ult}) \approx 0.615$. This led to premature failure in fatigue of the metal frame of the beam at $N \approx 41.74$ K cycles, which was associated with crack and delamination damages at the lower corner of the T.D. The frame was repaired by bolting the frame to the web and stiffening the flanges of the frame with metal strips (bolted to them). Then a residual strength test was carried out. It is seen from Table 3 that these damages slightly affected the residual strength of the web. During the course of the residual strength test of this web, it was also observed that its behavior on the way to failure and at failure was influenced by the damages and that it differed from either that of the "virgin" web 09B (which underwent an ultimate test only) or from that of the other webs in the present group. The modes of damage at $N = 41.74$ K cycles and after the residual strength test are shown in Fig. 12.

As a result of the premature failure of web 08A, the flanges of the beams in the present group were stiffened and the webs were bolted to the frames (in addition to being bonded) prior to their testing. Also, slightly lower working loads were chosen for webs 08B and 09A (see Table 3). Table 3 shows that both webs withstood the desired fatigue life of 250 K cycles. They experienced minor damages at the lower corner of the T.D. during the beginning of their fatigue life, but these damages were arrested after a while and therefore did not affect the endurance life of the webs. Table 3 reveals that the residual strength of these webs was affected to some extent as a result of the repeated bucklings at relatively high working load levels. The modes of damage and failure of web 09A are shown in Fig. 13.

Web 09B served to determine the ultimate load corresponding to the webs of beams 08 and 09. Its behavior on the way to failure and at failure was found to be similar to that experienced with web 09A in Fig. 13.

Beam HWB-10 was loaded with its outermost fibers in tension. As a result, the modes of damage experienced by web 10A of this beam differed completely from those observed in the previous webs of the present group. Delamination damages started at the lower corner of the T.D. after a relatively small number of cycles. This damage propagated along the T.D. towards the opposite corner of the T.D., and was fully developed at the end of the fatigue life of the web (see Fig. 14). The test results of web 10A in Table 3 show that the residual strength of this web was only slightly influenced by the above damages, but the behavior of the web on the way to failure and at failure differed from that of web 10B. It was similar to the behavior of the other webs in the present group.

Plots of responses of the webs of the present group, like those in Fig. 11, reveal similar behavior and tendencies to those experienced in the previous groups of beams, including the very high bending strain concentrations along the T.D., at its lower corner.

It should be noted that the webs in the present group exhibited some fatigue sensitivity, which in the case of web 09A resulted in as much as 15% degradation in the ultimate load carrying capacity.

The fourth group of beams in the present investigation had a $[\underline{\pm 45}]_s$ plane weave web and included beams HWB-11 and HWB-12. Plane weave material was used to eliminate the directionality tension/compression state of loading effect in the outermost fibers, which appeared in the webs in the previous groups.

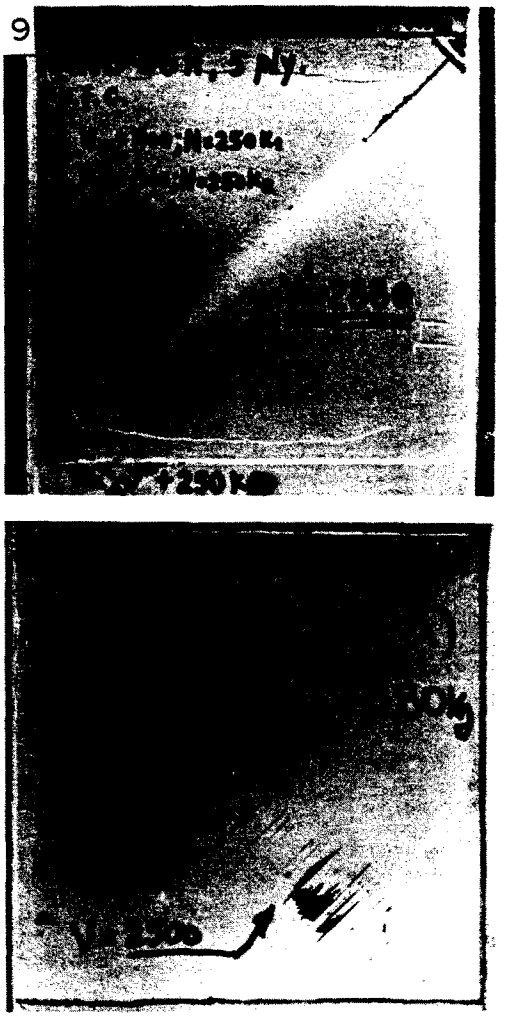

Fig. 9. Failure in residual strength test of shear web HWB-06A (after 250 K load cycles at V_{cyc} = 1100 kg and 1300 kg).

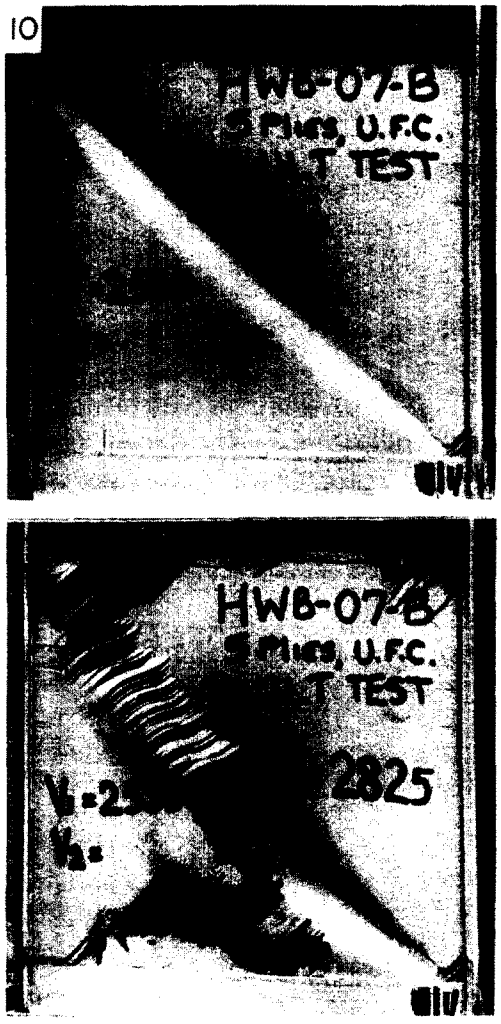

Fig. 10. Failure in ultimate test of shear web HWB-07B.

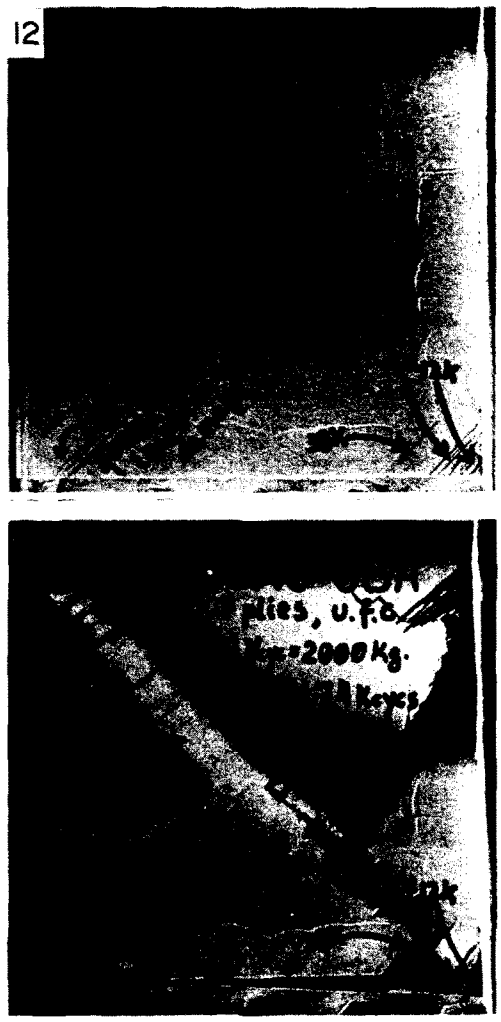

Fig. 12. Failure in residual strength test of shear web HWB-08A (after 41,740 load cycles at $V_{cyc} = 2000$ kg).

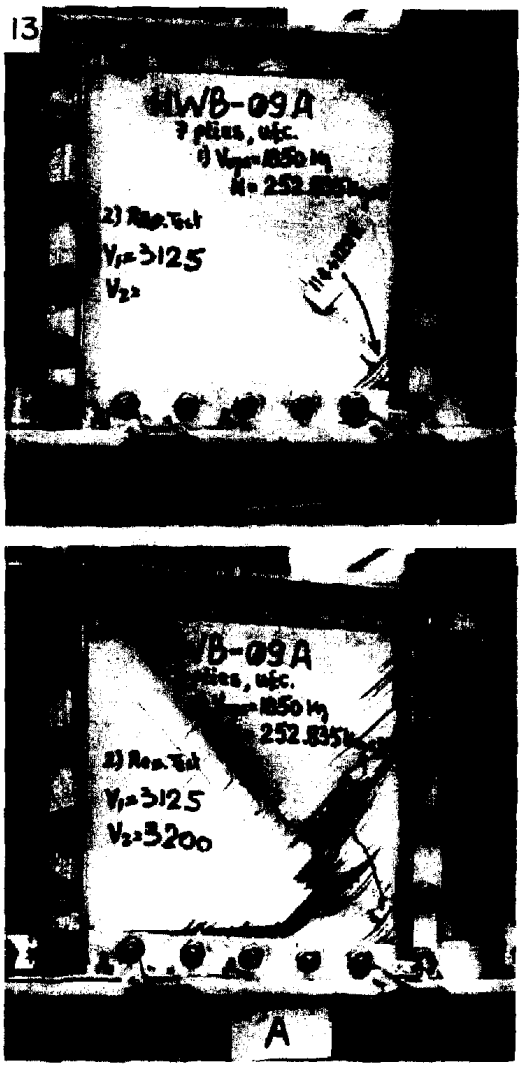

Fig. 13. Failure in residual strength test of shear web HWB-09A (after 252, 835 load cycles at $V_{cyc} = 1850$ kg).

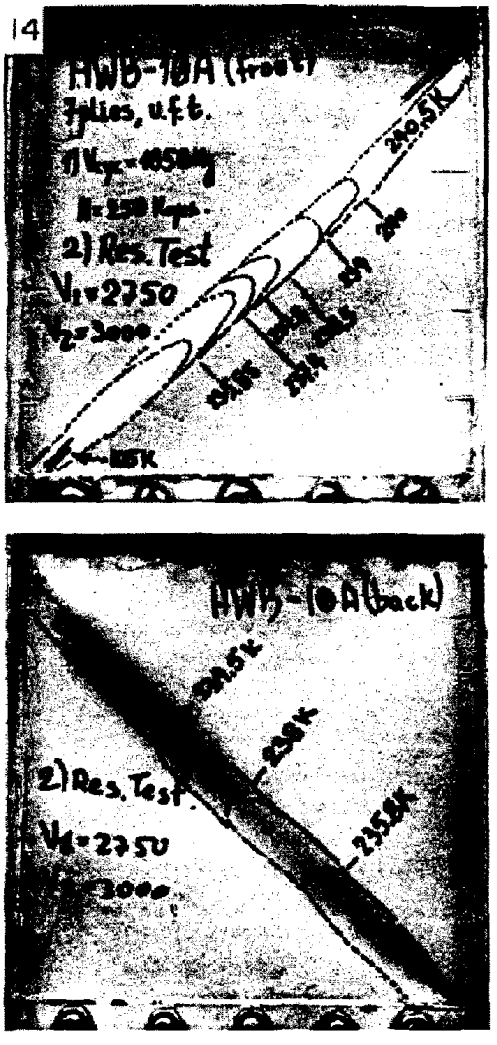

Fig. 14. Damage propagation in shear web HWB-10A (after 250 K load cycles at P_{cyc} = 1850 kg).

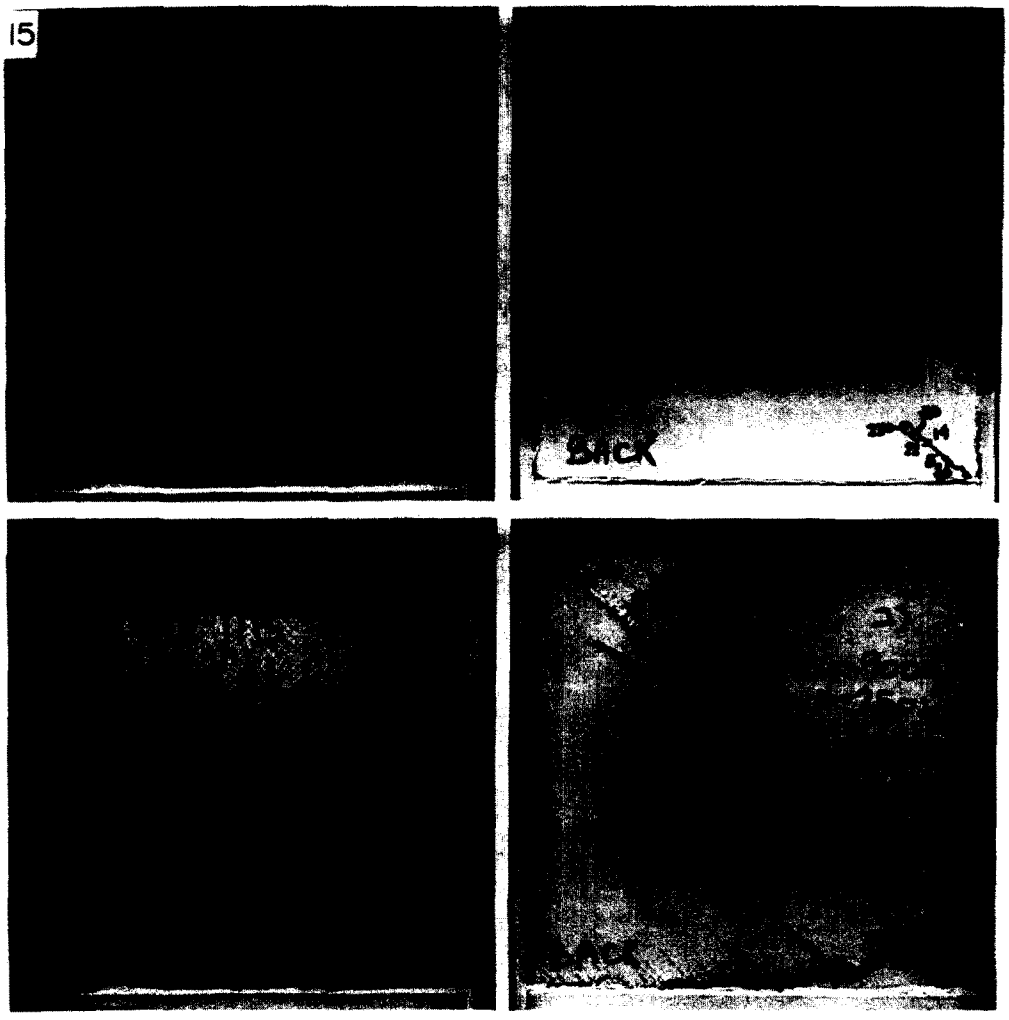

Fig. 15. Damage propagation and failure in residual strength test of shear web HWB-11B (after 250 K cyclic loadings at V_{cyc} = 900 kg).

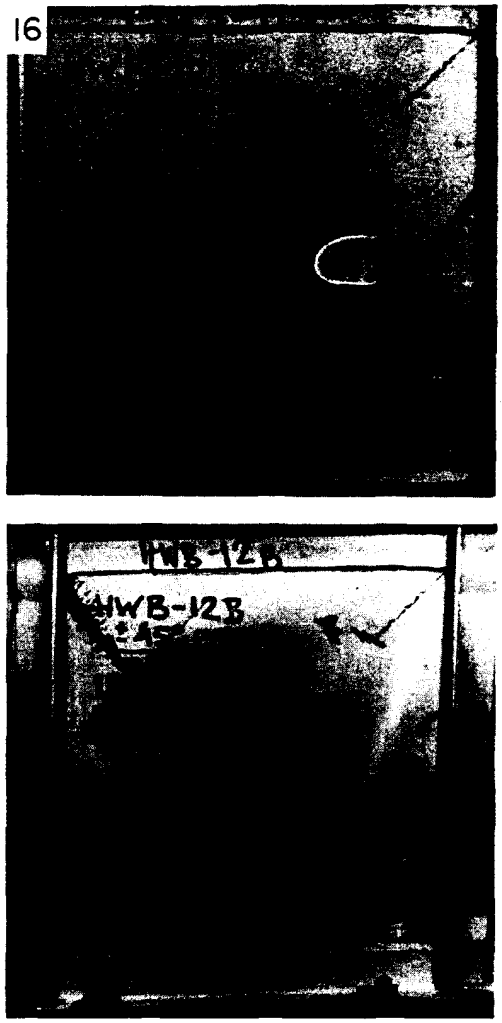

Fig. 16. Failure of shear web HWB-12B.

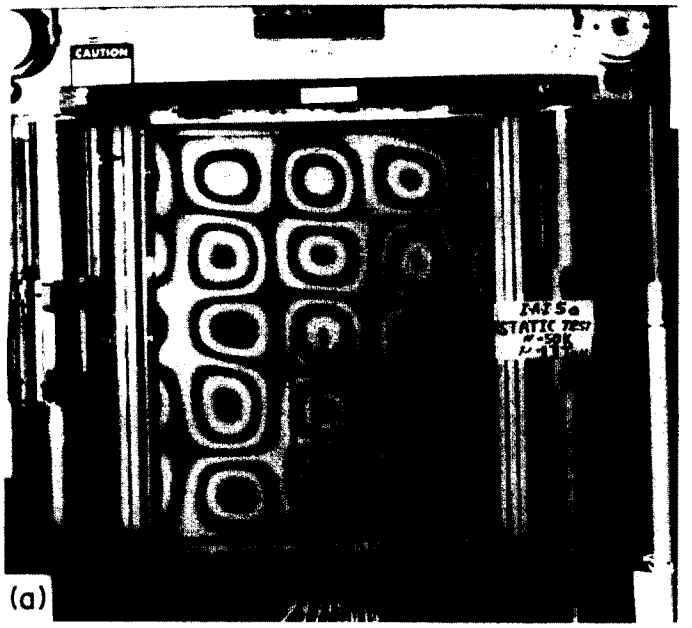

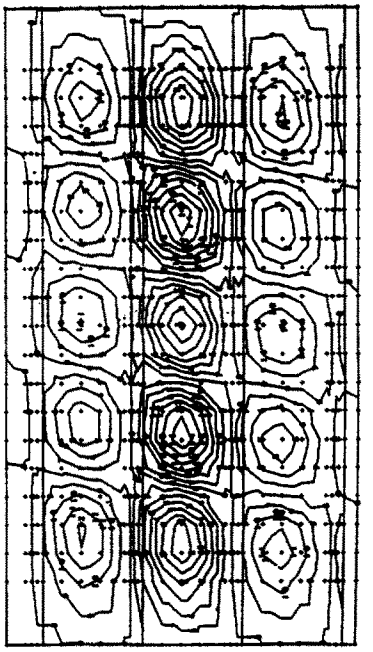

Fig. 18. Axial compression panel. (a) Moiré fringe pattern of skin buckling. (b) Computed wave pattern of skin buckling.

Fig. 21. Failure of axial compression panels. (a) Typical failure mode of panel *I*2. (b) Failure at the location of defects in panel *J*4.

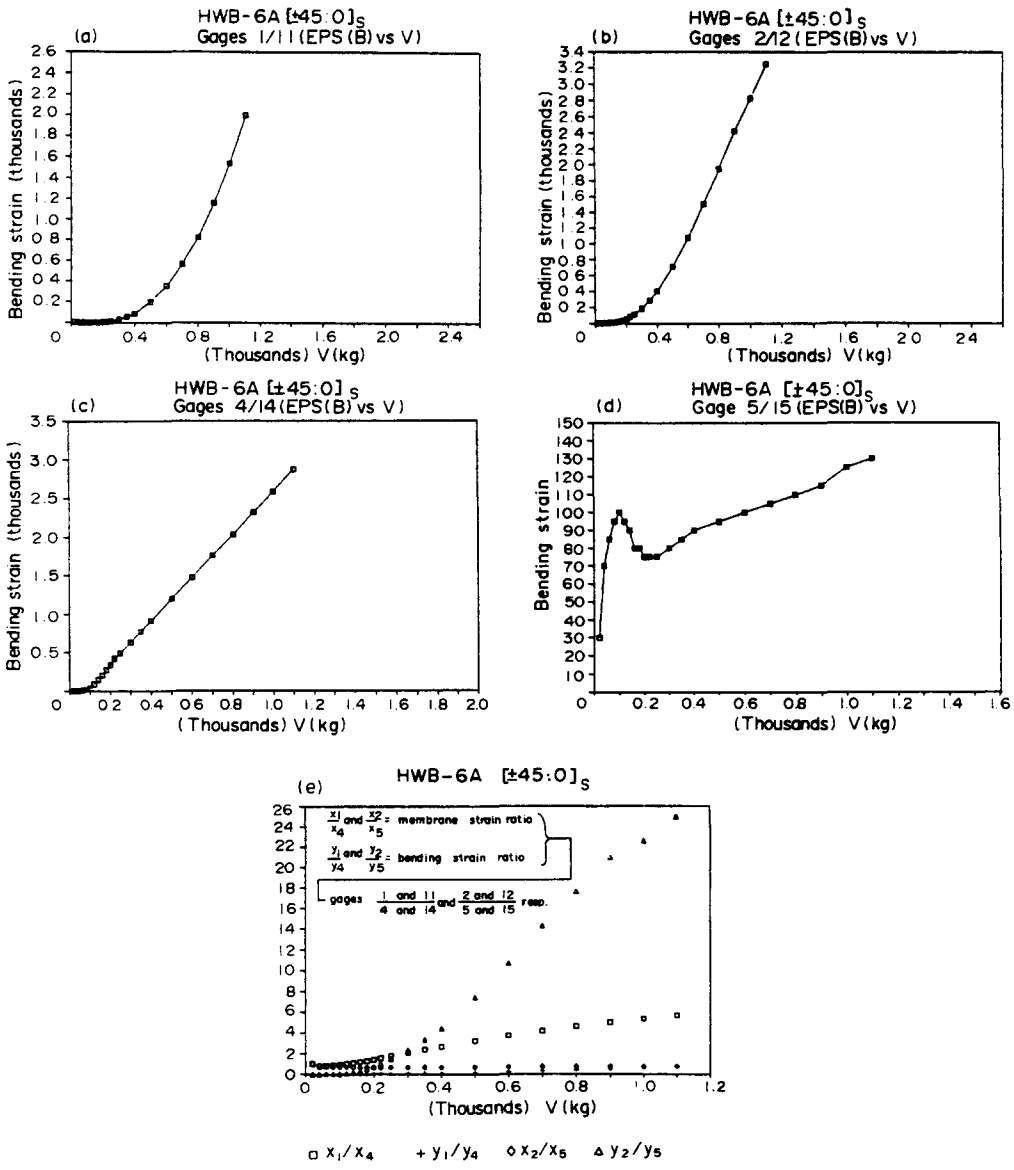

Fig. 11. Typical response curves for shear web HWB-6A. (a)–(d) Bending strain vs. load (gage locations given in Fig. 3). (e) Strain concentration.

The experimental critical loads of the webs in this group could not be determined satisfactorily from any of the strain/strain or strain/load responses.

Webs 11A, 11B and 12A underwent repeated buckling tests at different working load levels, $0.4 \leqslant (V_{cyc}/V_{ult}) \leqslant 0.55$. They all sustained their desired fatigue life of 250 K cycles and behaved very much alike during their load cycling. Damages developed in the form of cracks and delaminations along the T.D., cracks on the compression side of the web and delamination on the tension side. In the earlier life of the web these damages propagated along the T.D. and were arrested after a while. Their extent depended upon the working load level, V_{cyc} (see Fig. 15). It is seen in Table 3, that the residual strength of the webs was affected by the repeated buckling, and a load degradation of about 11% was experienced by web 11A. Also the behavior of these webs differed from that of the "intact" web 12B on the way to failure and at failure.

Web 12B was employed to determine the ultimate load of this group of webs. The mode of failure of the present layup is shown in Fig. 16.

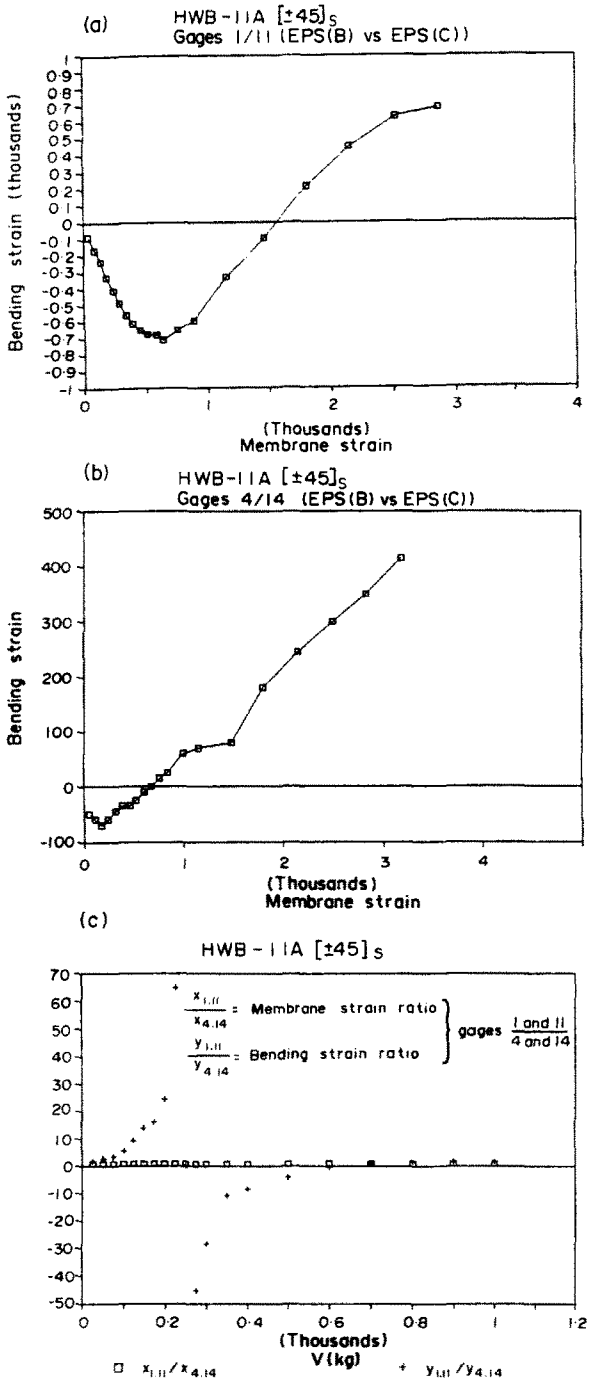

Fig. 17. Typical response curves of $[\pm 45]_s$ planeweave shear web HWB-11A. (a) and (b) Bending strain vs. membrane strain. (c) Strain concentration.

The typical response curves of the $[\pm 45]_s$ planeweave webs (Figs 17a, b and c) differ from those associated with the previous groups (Figs 11a–e). Like in the previous groups, high bending strain concentrations were experienced along the T.D. at the lower corner and are presented by Y1.11/Y4.14 in Fig. 17c. Unlike in other groups, there is a jump and change of direction in this curve. It should be noted that the group of planeweave webs also revealed some fatigue sensitivity, but their damage tolerance and margins of safety are high.

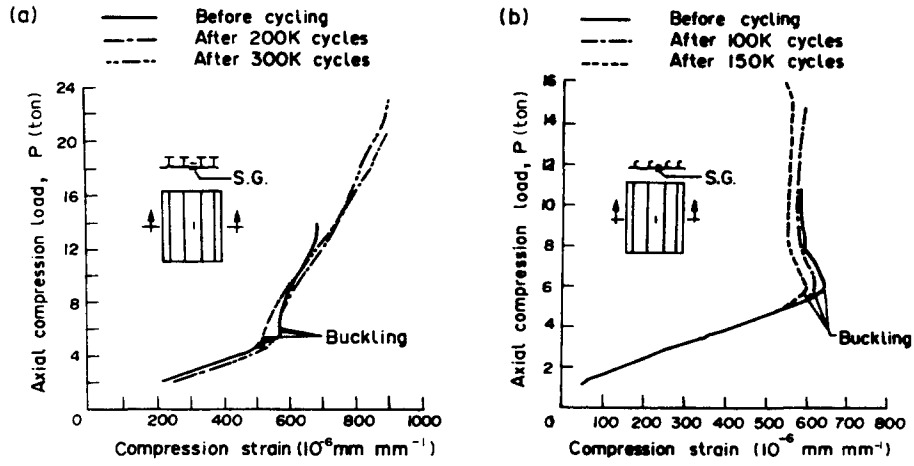

Fig. 19. Axial compression strains in center of skin. (a) Panel *I*2. Membrane strains at midspan in the skin of panel 2. (b) Panel *J*6. Membrane strains in central bay at mid-span panel 6.

4.2. *Axial compression panels*

The test results for the "*I*" and "*J*" panels and the corresponding calculated values are presented in Table 4. Local skin buckling was computed with NASTRAN MSC, PANDA 2 (Bushnell, 1987) and ESDU data sheets (E.S.D.U., 1980). Failure loads were calculated with PANDA 2 and as wide columns.

The skin buckled in both the "*I*" and "*J*" stiffened panels with five half-waves longitudinally and one transverse half-wave between each pair of stringers. A typical wave pattern obtained by the Moiré technique in the tests of a "*J*" stiffened panel, *J*5, is shown in Fig. 18, with the corresponding finite element (NASTRAN) buckling mode shape prediction. The experimental skin buckling loads were determined from plots of applied axial load vs axial membrane strain (like, e.g. Fig. 19), a method proposed originally by Hoff *et al.* (1948). Due to the usual difficulty of precise definition of the experimental critical load in an imperfect plate (with its stable postbuckling behavior) by this or any other method, there is considerable scatter in the experimental skin buckling loads in Table 4. The different methods of prediction also yield significantly different values in the Table. The PANDA 2 predictions, however, are closest to the average experimental values. The results shown in Table 4 and in Fig. 19 reveal that the buckling load was somewhat fatigue sensitive, and that there is a marked difference in the postbuckling behavior of the "*I*" and "*J*" stiffened panels.

In the postbuckling region, the usual change in load distribution, the large increase in load carrying share by the stiffeners, was observed for both types of panels (Segal *et al.*, 1987). However, contrary to the minor fatigue sensitivity of the skin buckling load, repeated buckling is not detrimental to the ultimate load carrying capacity of the panel. This can be seen in Fig. 20, showing the influence of load cycling on the axial compressive strain at a high load level. This is further reinforced by the column type tests carried out in Frostig *et al.* (1988).

Failure loads were predicted by PANDA 2 (Bushnell, 1987), and by the commonly used "wide column" analysis (including an effective width obtained from the test results), and are presented in Table 4. For the "*I*" stiffened panels the "wide column" predictions are in good agreement with the average experimental loads, whereas for the "*J*" stiffened panels the calculated loads are significantly higher than the experimental ones. The PANDA 2 predictions, both for simple and clamped supports, bound the experimental results. It should also be noted that failure was not caused by stiffener buckling in any of the panels tested (Segal *et al.*, 1987).

Manufacturing defects, mainly porosity, did not affect the initial buckling, but final failure loads were affected by them, as well as by geometrical imperfections (Segal *et al.*, 1987). Final failure of all the panels was initiated at the stiffener caps and spread across the

Table 4. Panel loading, skin buckling and ultimate/residual strength

Panel type and number	Cyclic load range [ton]	Total number of cycles [kilocycles]	Local skin buckling [ton]							Failure and residual loads [ton]			
			Computed					Experimental		Computed			
			NASTRAN MSC	E.S.D.U. (1980)		PANDA 2 Bushnell (1987)				Wide column including effective width	PANDA 2 Bushnell (1987)		
				Simply supported	Clamped	Simply supported	Clamped	Before cycling	After 250 K cycles		Simply supported	Clamped	Experimental
*I*1	Static	—	7.1	4.98	7.97	5.5	5.6	5.35	—	36.2	19.1	50.2	24.0
*I*2	14–22	315	7.1	4.98	7.97	5.5	5.6	5.80	5.20	36.2	19.1	50.2	32.0
*I*3	15–21	250	7.1	4.98	7.97	5.5	5.6	7.00	6.20	36.2	19.1	50.2	33.5
*J*4	Static	—	5.15	3.82	6.11	4.4	4.45	3.40	—	22.4	14.0	20.5	15.0
*J*5	11–12	75*	5.15	3.82	6.11	4.4	4.45	4.50	—	22.4	14.0	20.5	*
*I*6	11–15	250	5.15	3.82	6.11	4.4	4.45	6.05	5.00	22.4	14.0	20.5	16.7

* Panel broke during loading due to loading machine failure.

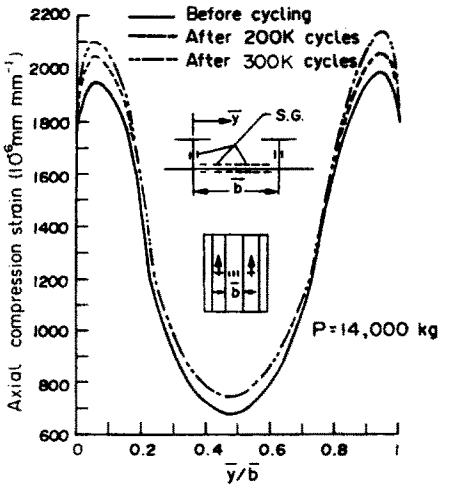

Fig. 20. Influence of repeated buckling on the axial compression in panel *I2* (*P* in tons). Cyclic loading effects on membrane strains distribution of skin in panel 2.

skin along 45 degree lines. A typical failure is shown in Fig. 21a. Panels which contained manufacturing defects in the caps broke at the location of the defects as can be seen in Fig. 21b. No damage or failure occurred at the stiffener-skin interface as was the case in Romeo (1986). Final failure load of most panels ranged between 4.4 to 5.5 times their initial buckling load.

5. CONCLUSIONS

(1) Composite stiffened panels can be safely utilized in the "deep" postbuckling region also under repeated loading. This was shown conclusively by the postbuckling and failure behavior of both the shear panels and compression panels.

(2) All shear and compression panels sustained the specified fatigue life of 250,000 cycles.

(3) In most of the *shear panels* significant damages developed with increasing number of repeated buckling cycles, the extent of the damage depending on the working load level, V_{cyc}. But, no matter how pronounced the damage was, it did not affect the fatigue life of the panels; even extensive delamination did not result in immediate catastrophic failure. The residual strength of the panels was reduced, however, by up to 20%. In the static tests, two ultimate loads were observed, the final one being 10–20% higher.

The correct placement of the outer fibers in the stacking sequence of the web was found to be of great importance. Placing these fibers in the tension field direction increased the ultimate shear strength.

Comparison of the composite shear web test results with those of the corresponding metal shear webs of the earlier investigations (Weller *et al.*, 1984b; Libai *et al.*, 1984), shows the advantages of the composite webs, primarily less sensitivity to fatigue at similar levels of cyclic working loads.

(4) All the *compression panels* were of the relatively "heavy" stiffener type, where the skin buckled first with stiffeners (with an effective width of skin) failing at a load 4.5 to 5.5 times the initial skin buckling load. The initial buckling was somewhat reduced by repeated buckling, whereas the ultimate load carrying capability of the stiffened panel was not affected and often even slightly increased.

Panel failure initiated at the stiffener caps of one of the outer stiffeners, followed by failure of the two central stiffeners, these failures being associated with 45° cracks in the skin (parallel to the 45° fibers in the outer plies, see Fig. 21).

No stiffener separation from skin was experienced. This failure mode was prevented by overlapping the last two upper plies in the skin on the flange and by manufacturing the panel in one stage. Thus the development of interlaminar shear stress was eliminated and the effect of peeling stresses at flange-skin intersection reduced.

Note that the test results indicate that "*I*" stiffened compression panels, though weighing more than the corresponding "*J*" stiffened ones, are structurally more efficient.

Comparison between PANDA 2 (Bushnell, 1987), type predictions and test results verify the suitability of PANDA 2 for initial sizing of flat composite compression panels.

(5) The two repeated buckling test programs on stiffened shear panels and stiffened axial compression panels showed clearly less fatigue sensitivity of the composite (Graphite/Epoxy) panels. This feature adds to other advantages of composite structures.

Safe design of stiffened Graphite/Epoxy panels well beyond their initial buckling is therefore feasible, which will result in their increased structural efficiency.

Acknowledgements—The authors wish to express their gratitude to Israel Aircraft Industries and United States Air Force Office of Scientific Research for sponsoring parts of the present research, to the staff of the Aeronautical Structures Laboratory, Messrs A. Grunwald, S. Nachmani and B. Levi, for their assistance during the course of the tests, to Prof. A. Libai for valuable discussions and to Mrs B. Hirsch for typing the manuscript.

REFERENCES

Agarwal, B. L. (1981). Postbuckling behavior of composite shear webs. *AIAA J.* **19**(7), 933–939.

Agarwal, B. L. (1982). Postbuckling behavior of composite-stiffened curved panels in compression. *Exp. Mech.* **22**, 231–236.

Almroth, B. D., Brogan, F. A., Meller, E., Zele, F. and Petersen, H. T. (1973). Collapse analysis for shells of general shape: user's manual for the STAGS-A computer code. AFFDL TR-71-8.

Ari-Gur, J., Singer, J. and Libai, A. (1982). Repeated buckling tests of stiffened thin shear panels. *Israel J. Tech.* **20**, 220–231.

Ashton, J. E. and Whitney, J. M. (1970). *Theory of Laminated Plates.* Progress in Materials Science Series, Vol. IV, pp. 61–63.

Bushnell, D. (1987). PANDA 2—Program for minimum weight design of stiffened, composite, locally buckled panels. *Comp. Struct.* **25**(4), 469–605.

Deo, R. B. (1985). Design development and durability validation of postbuckling composite and metal panels. *Tech. Assess.* AFWAL TR-85-3077.

Deo, R. B. and Agarwal, B. L. (1985). Design methodology and life analysis of postbuckled metal and composite panels. *Design Guide* AFWAL TR-85-3096.

E.S.D.U. (1980). Buckling of rectangular specially orthotropic plates. *Engng. Sci. Data* Vol. 8, Item No. 80023. Engineering Science Data Unit, London.

Faulkner, D. (1975). A review of effective plating for use in the analysis of stiffened plating in bending and compression. *J. Ship Res.* **19**(1), 1–17.

Frostig, Y., Siton, G., Segal, A., Sheinman, I. and Weller, T. (1988). Postbuckling behavior of laminated composite stiffeners and stiffened panels under cyclic loading. In *ICAS 1988, Proceedings of the 16th Congress of the International Council of Aeronautical Sciences.* pp. 931–944. Jerusalem, Israel.

Frostig, Y., Siton, G., Segal, A., Sheinman, I. and Weller, T. (1989). Postbuckling of flat stiffened GR/EP panels under cyclic compression. *To be Presented at the 3rd ECCM Conf. on Composite Materials.* Bordeaux, France.

Hoff, N. J., Boley, B. and Coan, M. (1948). The development of a technique for testing stiff panels in edgewise compression. *Proc. Soc. of Experi. Stress Anal.* **5**(2), 14–24.

Knight, N. F., Jr. and Starnes, J. H., Jr. (1985). Postbuckling behavior of selected curved stiffened graphite-epoxy panels loaded in axial compression. *Trans. ASME, J. Pres. Ves. Tech.* **107**(4), 394–402.

Kollet, M., Weller, T., Libai, A. and Singer, J. (1983) Durability under repeated buckling of stiffened shear panels. Tech.—Israel Inst. Tech. Dept. of Aeronaut. Engng. TAE Report No. 509.

Kudva, N. J. and Agarwal, B. L. (1981). Postbuckling analysis of stiffened composite shear panels—theoretical analysis and comparisons with experiments. In *Advances in Aerospace Structures and Materials, Proceedings of the 102 ASME Winter Annual Meeting.* pp. 221–229.

Kuhn, P., Peterson, J. P. and Levin, L. R. (1952). A summary of diagonal tension. Part I—*Methods of Analysis.* NACA TN 2661.

Libai, A., Weller, T., Kollet, M. and Singer, J. (1984). Stiffened panels subjected to repeated buckling—durability studies. Tech.—Israel Inst. Tech. Dept. of Aeronaut. Engng. TAE Report No. 545.

Renieri, M. P. and Garrett, R. A. (1981a). Postbuckling behavior of flat stiffened graphite/epoxy shear panels. MCAIR Rep. No. 81-015. McDonnell Aircraft Company, St. Louis, Missouri.

Renieri, M. P. and Garrett, R. A. (1981b). Investigation of the local buckling, postbuckling and crippling behavior of graphite/epoxy short thin-walled compression members. Report MDC A7091. McDonnell Aircraft Company, St. Louis, Missouri.

Rockey, K. C. (1977). The design of web plates for plate and box girders—A state of the art report. In *Steel Plated Structures* (Edited by P. J. Dowling, J. E. Harding and P. E. Frieze), pp. 459–485. Crosby Lockwood Staples, London.

Romeo, G. (1986). Experimental investigation on advanced composite-stiffened structures under uniaxial compression and bending. *AIAA J.* **24**(11), 1823–1830.

Rouse, M. (1987). Postbuckling and failure characteristics of stiffened graphite-epoxy shear webs. Paper No. 87-0733. In *Proceedings of the AIAA/ASME/ASCE/AHS 28th SDM Conference.* pp. 181–193. Monterey, California.

Segal, A., Siton, G. and Weller, T. (1987). Durability of graphite/epoxy stiffened panels under cyclic postbuckling compression loading. In *Proceedings ICCM & ECCM, 6th International Conf. on Composite Materials and 2nd*

European Conf. on Composite Materials (Edited by F. L. Mathews, N. C. R. Bushnell, J. H. Hodgkinson and J. Morton), pp. 5.69–5.78. Imperial College, London, England.

Spier, E. E. (1975). Crippling/column buckling analysis and test of graphite/epoxy stiffened panels. *AIAA J.* **13**(1), 1–16.

Starnes, J. H., Jr., Knight, N. F. and Rouse, M. (1985). Postbuckling behavior of selected flat stiffened graphite-epoxy panel loaded in compression. *AIAA J.* **23**(8), 1236–1246.

Vestergren, P. and Knutsson, L. Theoretical and experimental investigation of the buckling and postbuckling characteristics of flat carbon fiber reinforced plastic (CFRP) panels subjected to compression or shear loads. In *ICAS 1978, Proceedings of the 11th Congress of the International Council of Aeronautical Sciences* (Edited by J. Singer and R. Staufenbiel), pp. 217–223. Lisboa, Portugal.

Von Karman, T., Sechler, E. E. and Donnell, L. H. (1932). The strength of thin plates in compression. *ASME Transactions* **64**(2), 53–57.

Wagner, H. (1929). Ebene Blechwandträger mit sehr dünnem Stegblech. Zeitschrift für Flugtechnik und Motorluftsch. **20** (8–12); translation: Flat sheet metal girders with very thin metal web. NACA TM, 604–606.

Weller, T., Kollet, M., Libai, A. and Singer, J. (1984a). Durability under repeated buckling of stiffened shear panels. In *ICAS 1984, Proceedings of the 14th Congress of the International Council of the Aeronautical Sciences* (Edited by B. Laschka and R. Staufenbiel), pp. 932–942. *International Council of the Aeronautical Sciences.* Tolouse, France. *Synoptic in J. of Aircraft* **24**(1), 6–7 (1987).

Weller, T., Messer, G. and Libai, A. (1984b). Repeated buckling of graphite epoxy shear panels with bonded metal stiffeners, TAE Report No. 546. Dept. of Aeronautical Engng. Tech.—Israel Inst. of Tech. Haifa, Israel.